Electronic Supplementary Material (ESI) for Green Chemistry.

Supporting information

Engineering cellulose into water soluble poly(protic ionic liquids) electrolytes in DBU/CO_2/DMSO solvent system as organocatalyst for Knoevenagel condensation reaction

Yuqing Shen, Chaoping Yuan, Xianyi Zhu, Qin Chen, Shenjun Lu, Haibo Xie*

Department of polymer materials and engineering, College of Materials and Metallurgy, Guizhou University, Guiyang, 550025, China

Email: hbxie@gzu.edu.cn

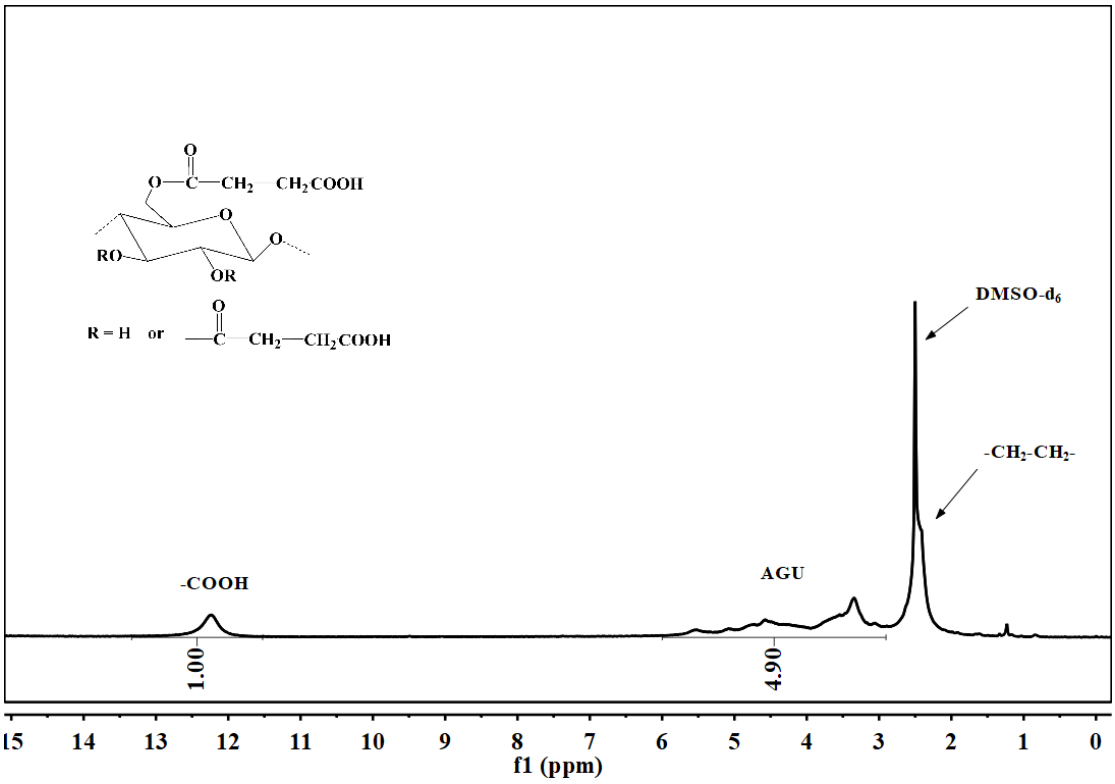

Figure S1. ^{1}H NMR (DMSO-d_6) spectrum of CSMEA (C-1, DS =1.43).

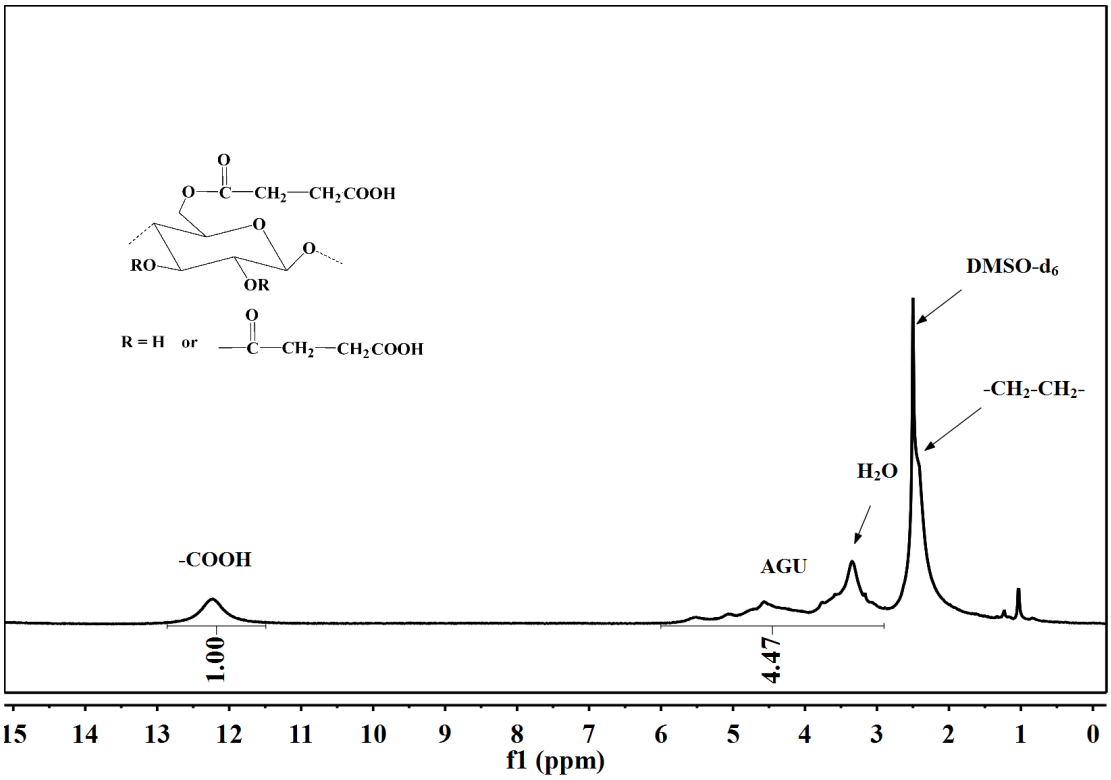

Figure S2. ^{1}H NMR (DMSO-d$_6$) spectrum of CSMEA (C-2, DS =1.57).

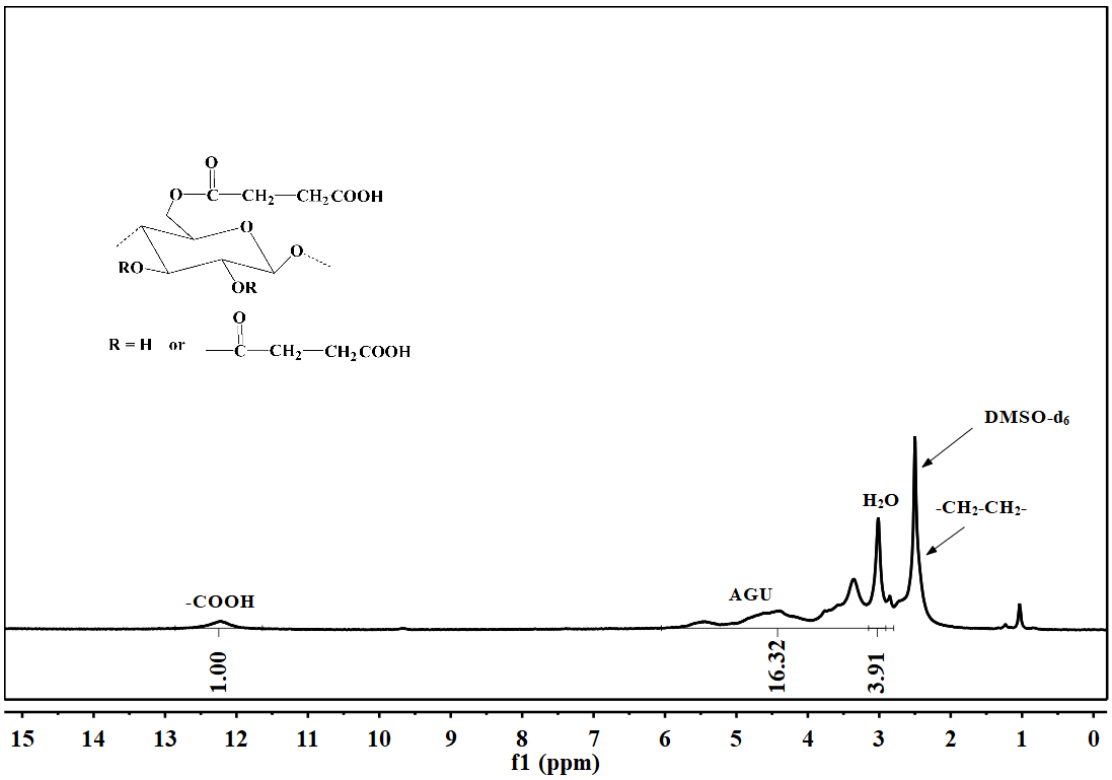

Figure S3. ^{1}H NMR (DMSO-d$_6$) spectrum of CSMEA (C-3, DS =0.56).

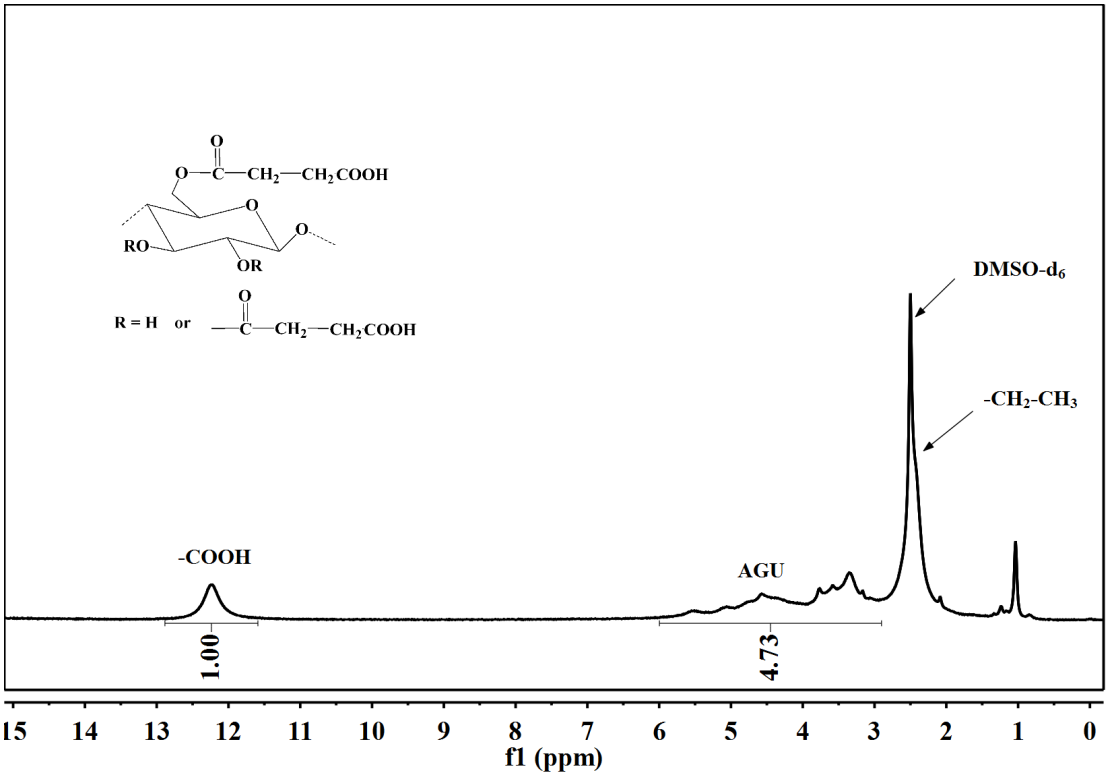

Figure S4. ^{1}H NMR (DMSO-d$_6$) spectrum of CSMEA (C-4, DS =1.48).

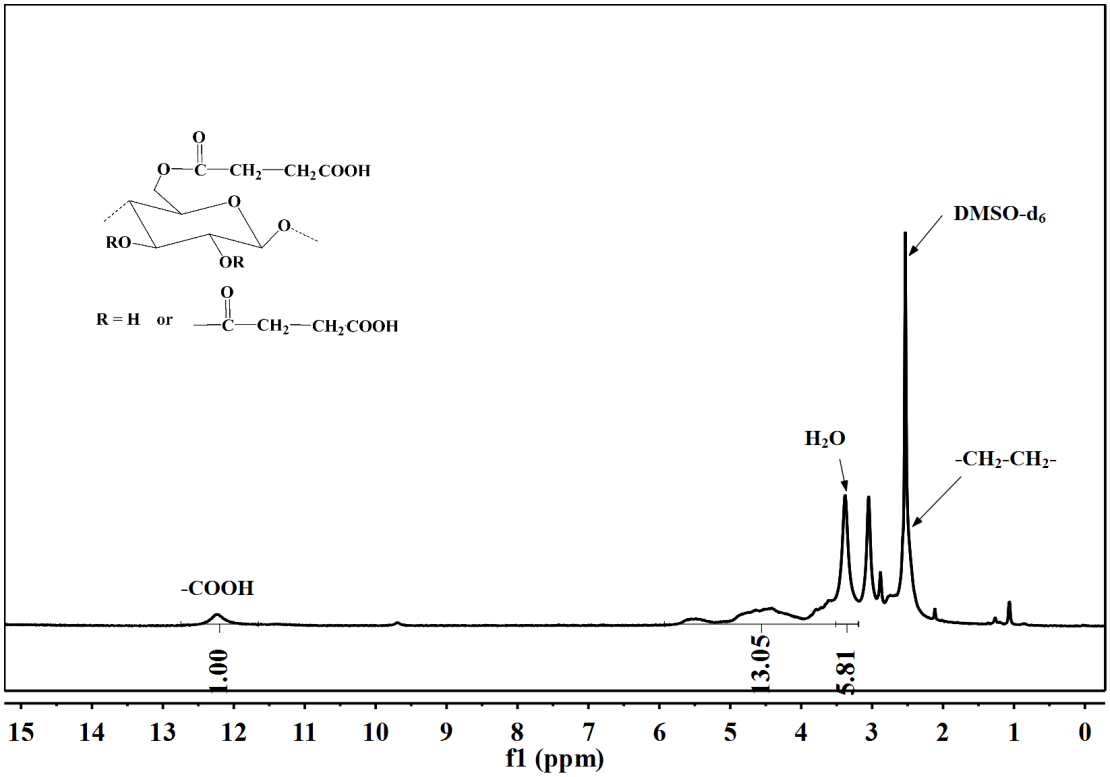

Figure S5. ^{1}H NMR (DMSO-d$_6$) spectrum of CSMEA (C-5, DS =0.97).

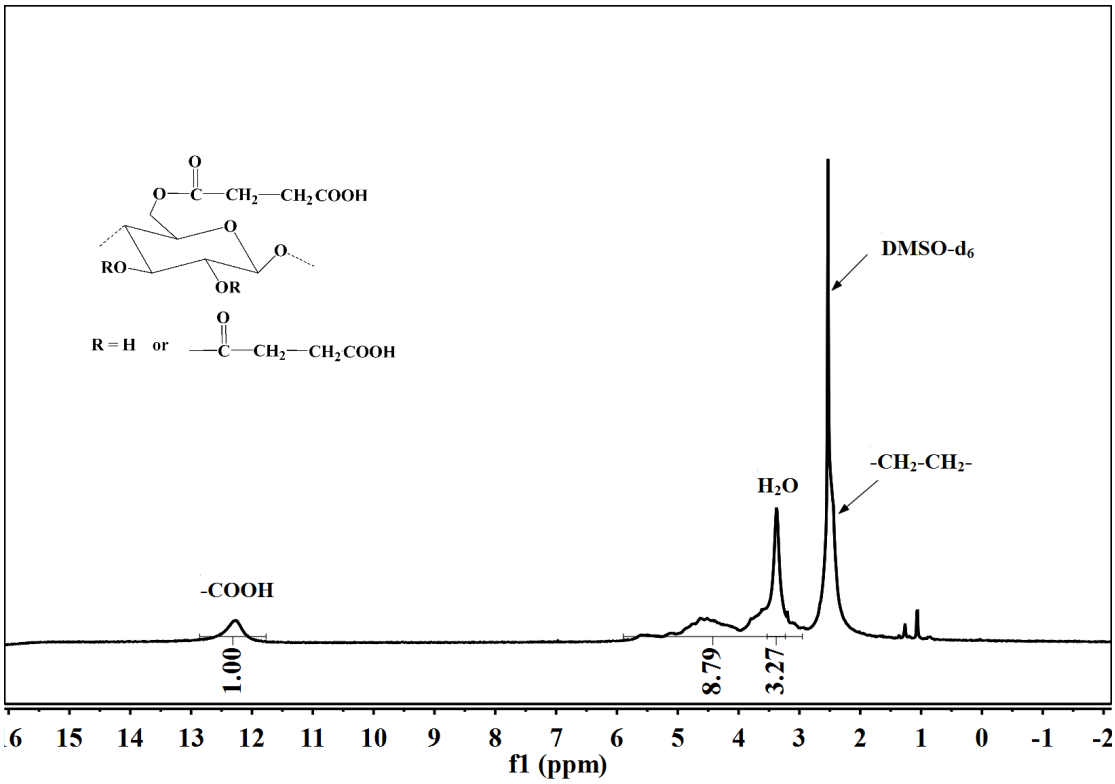

Figure S6. ^{1}H NMR (DMSO-d$_6$) spectrum of CSMEA (C-6, DS =1.27).

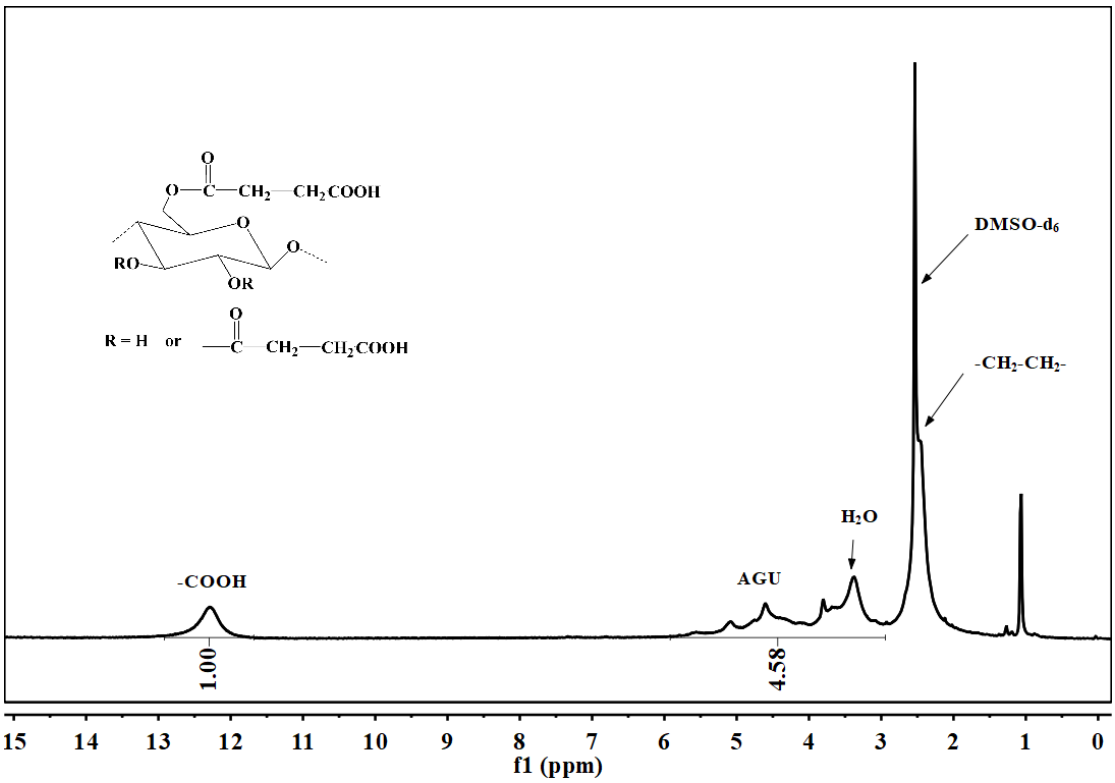

Figure S7. ^{1}H NMR (DMSO-d$_6$) spectrum of CSMEA (C-7, DS =1.53).

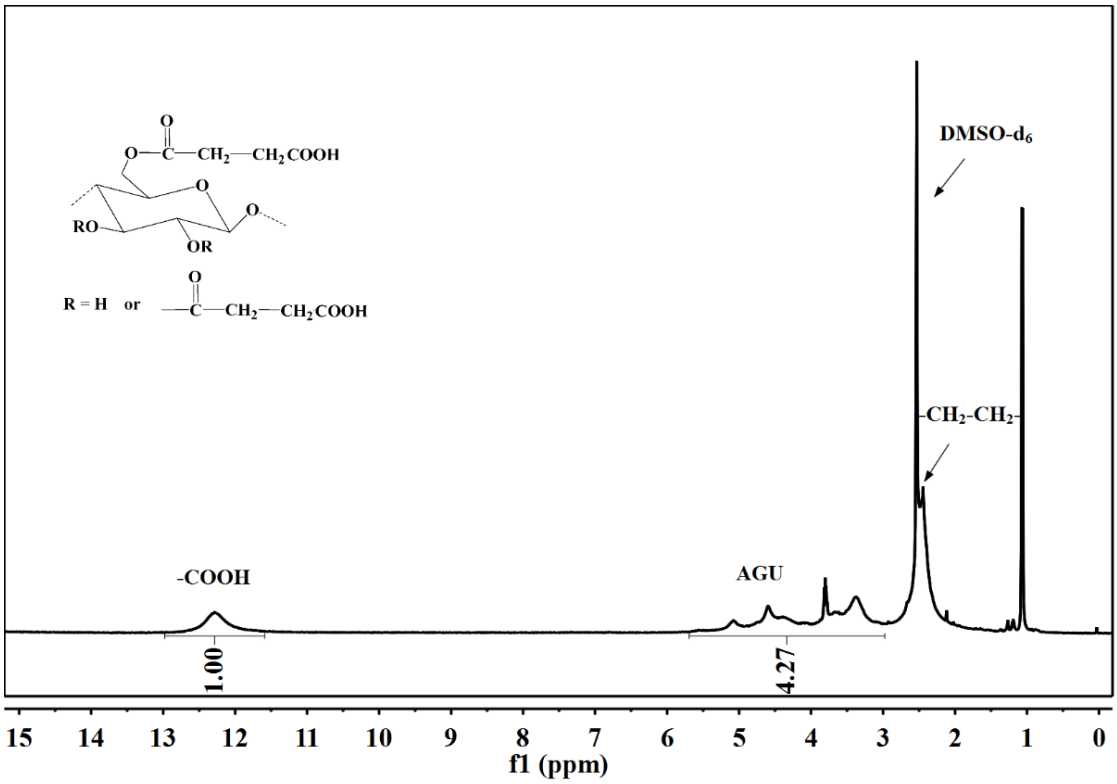

Figure S8. ^{1}H NMR (DMSO-d$_6$) spectrum of CSMEA (C-8, DS =1.64).

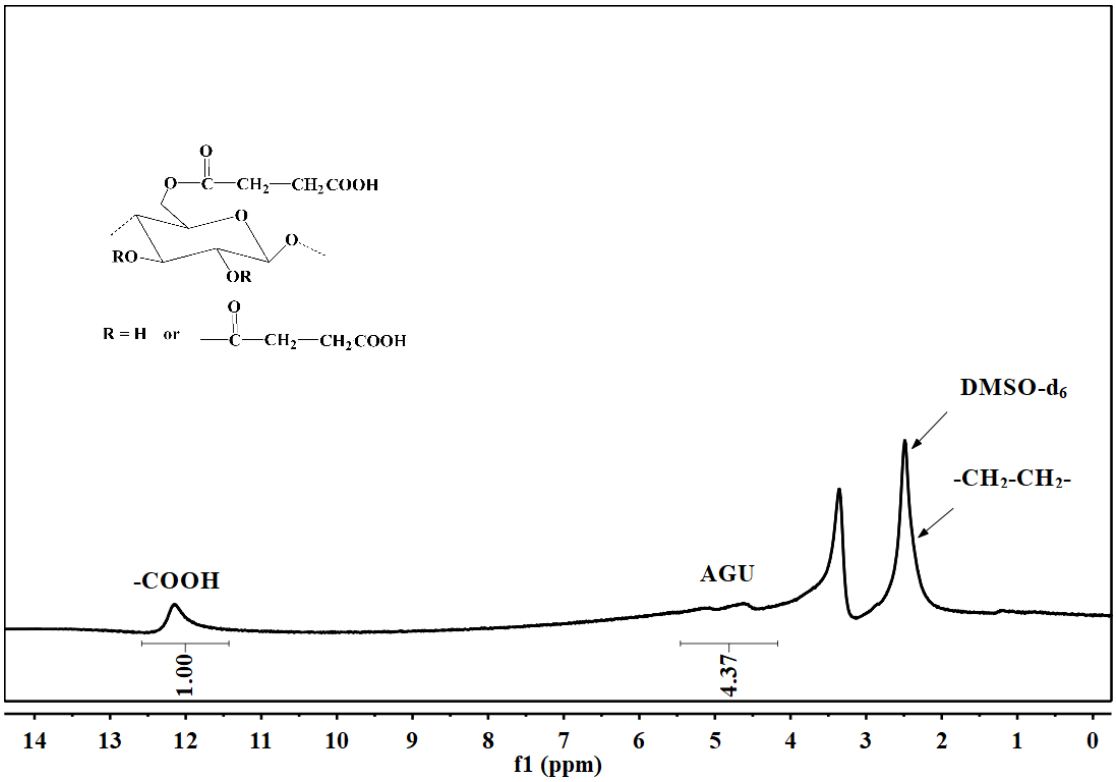

Figure S9. ^{1}H NMR (DMSO-d$_6$) spectrum of CSMEA (C-9, DS =1.60).

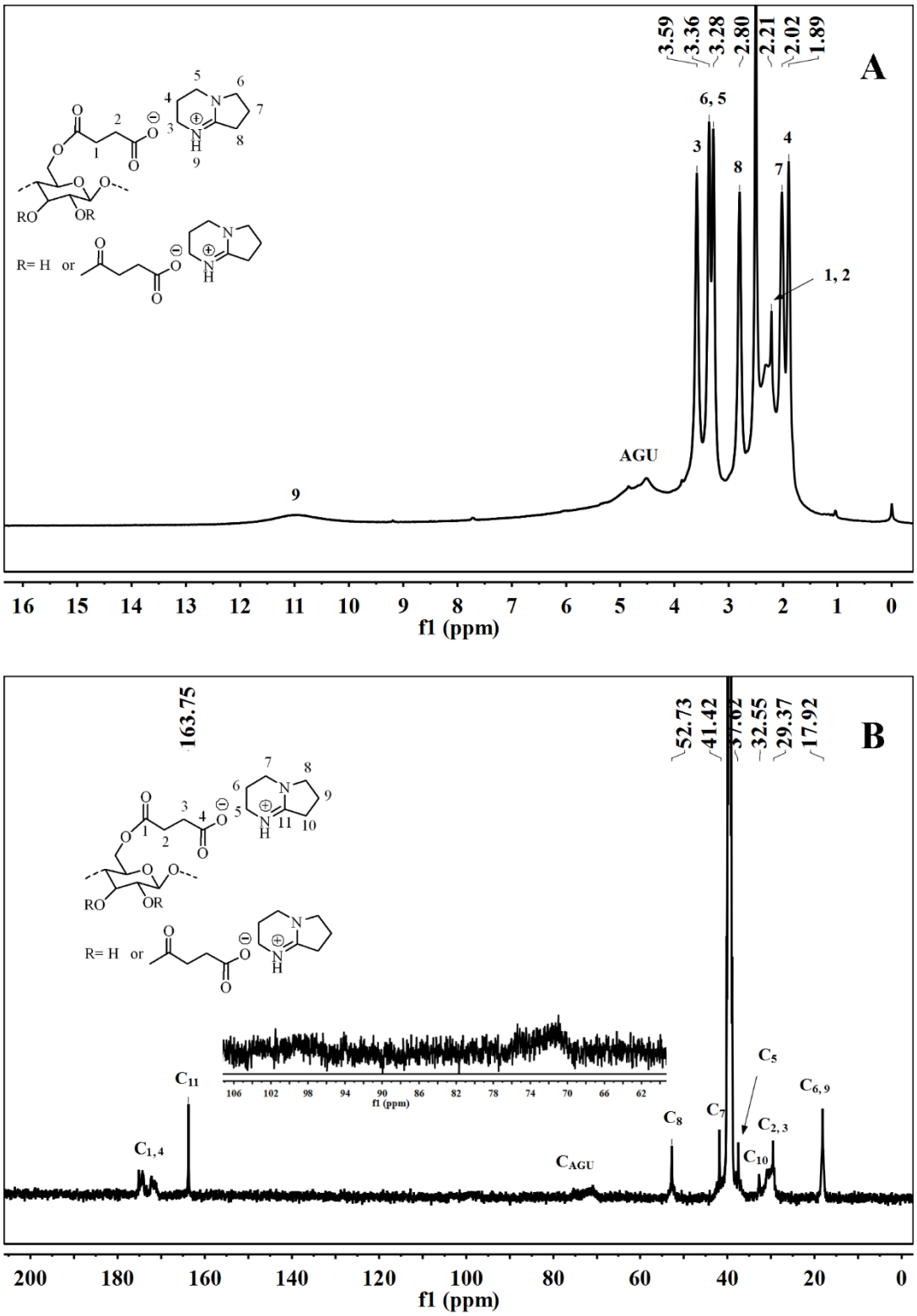

Figure S10. NMR (DMSO-d_6) spectra of CPIL (C-10, DS=0.51): (A) ^{1}H NMR, (B) ^{13}C NMR.

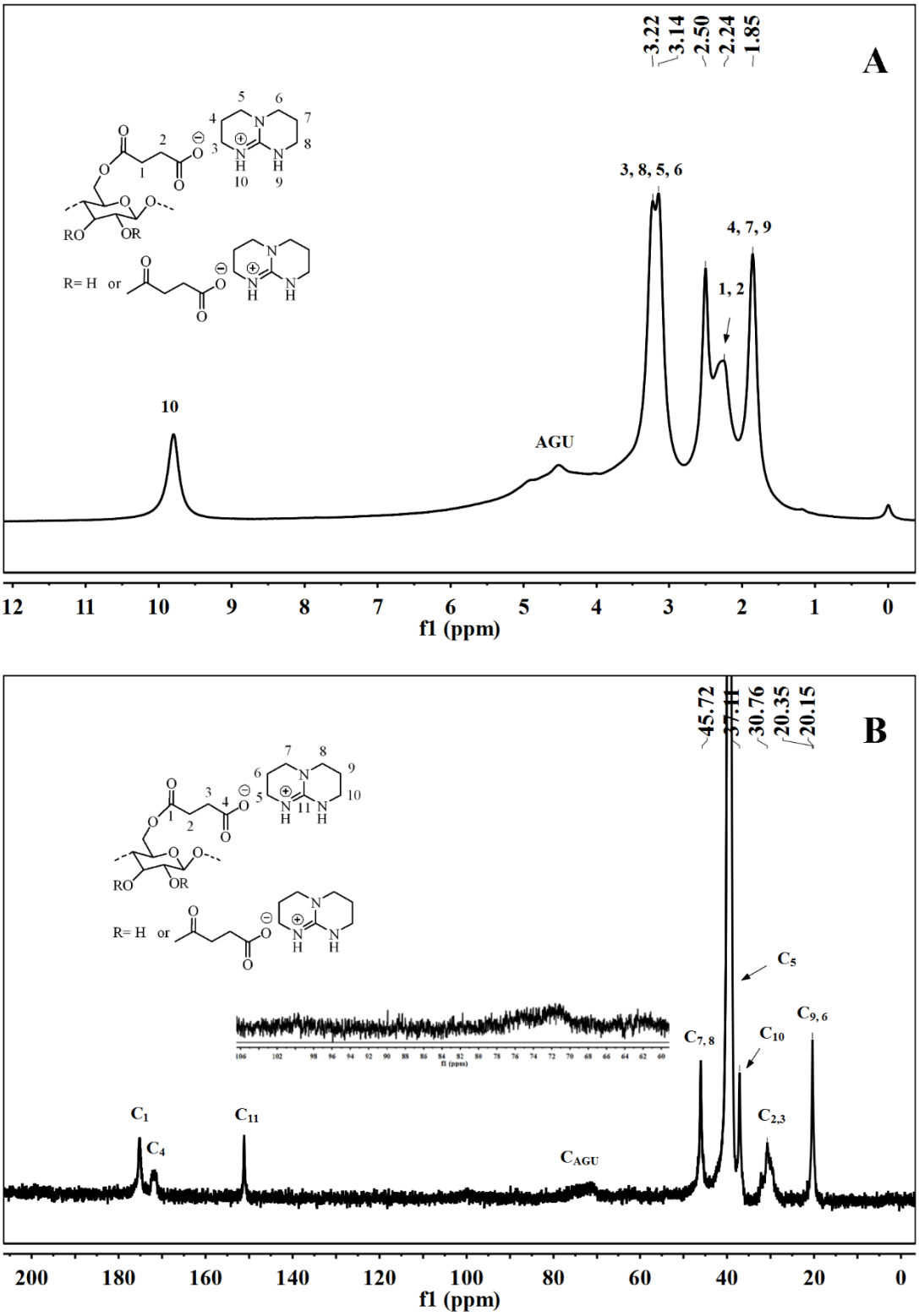

Figure S11. NMR (DMSO-d_6) spectra of CPIL (C-11, DS=0.90): (A) $_1$H NMR, (B) $_{13}$C NMR.

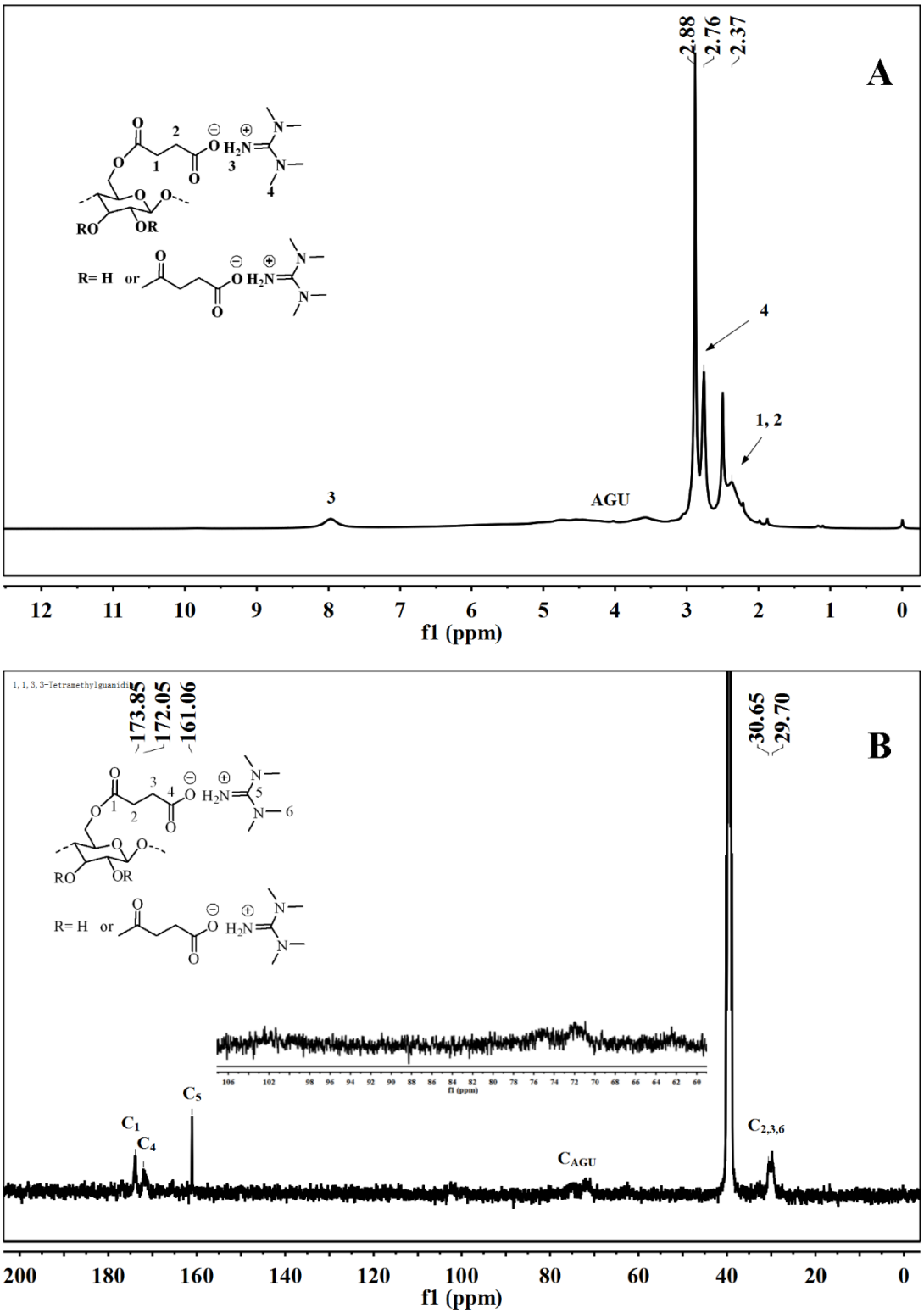

Figure S12. NMR (DMSO-d_6) spectra of CPIL (C-12, DS=0.36): (A) $_1$H NMR, (B) $_{13}$C NMR.

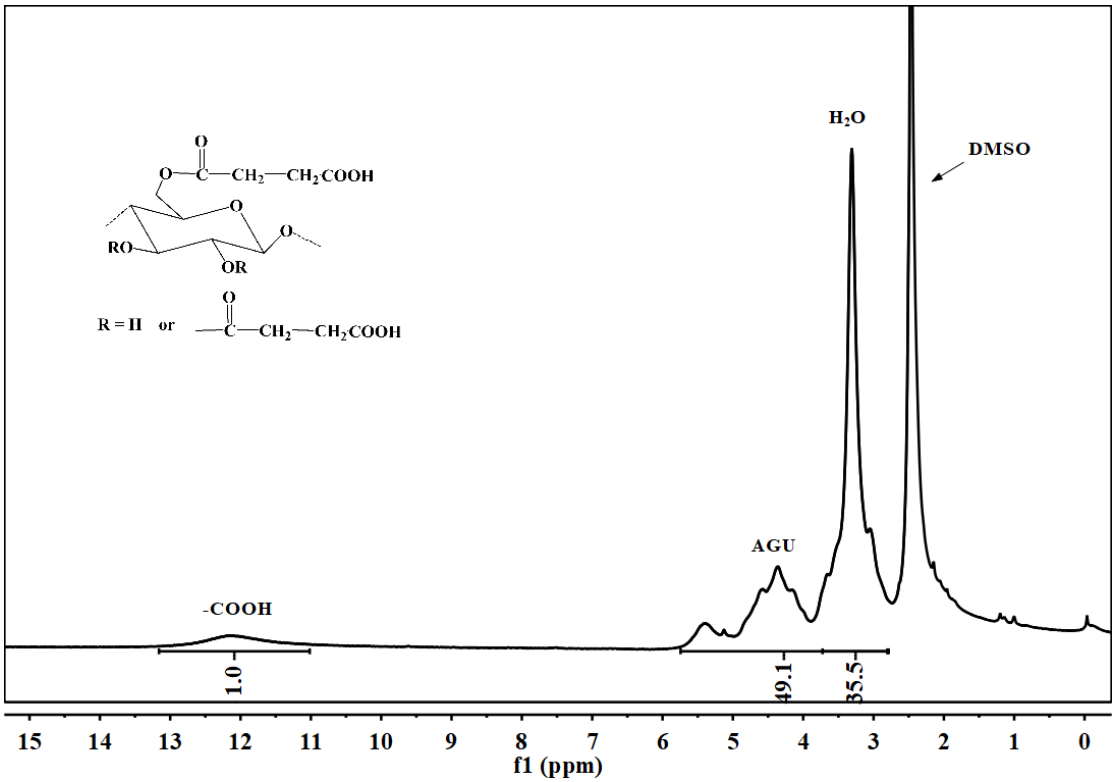

Figure S13. ^{1}H NMR (DMSO-d$_6$) spectrum of CSMEA (C-10, DS =0.51).

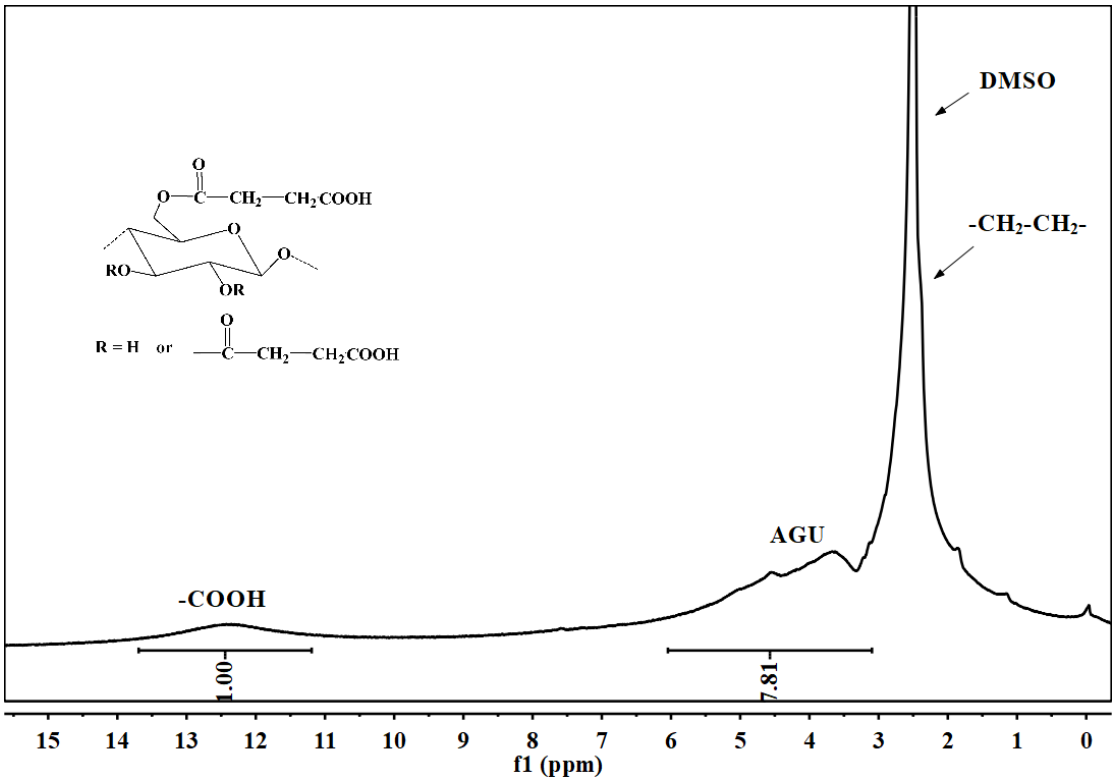

Figure S14. ^{1}H NMR (DMSO-d$_6$) spectrum of CSMEA (C-11, DS =0.90).

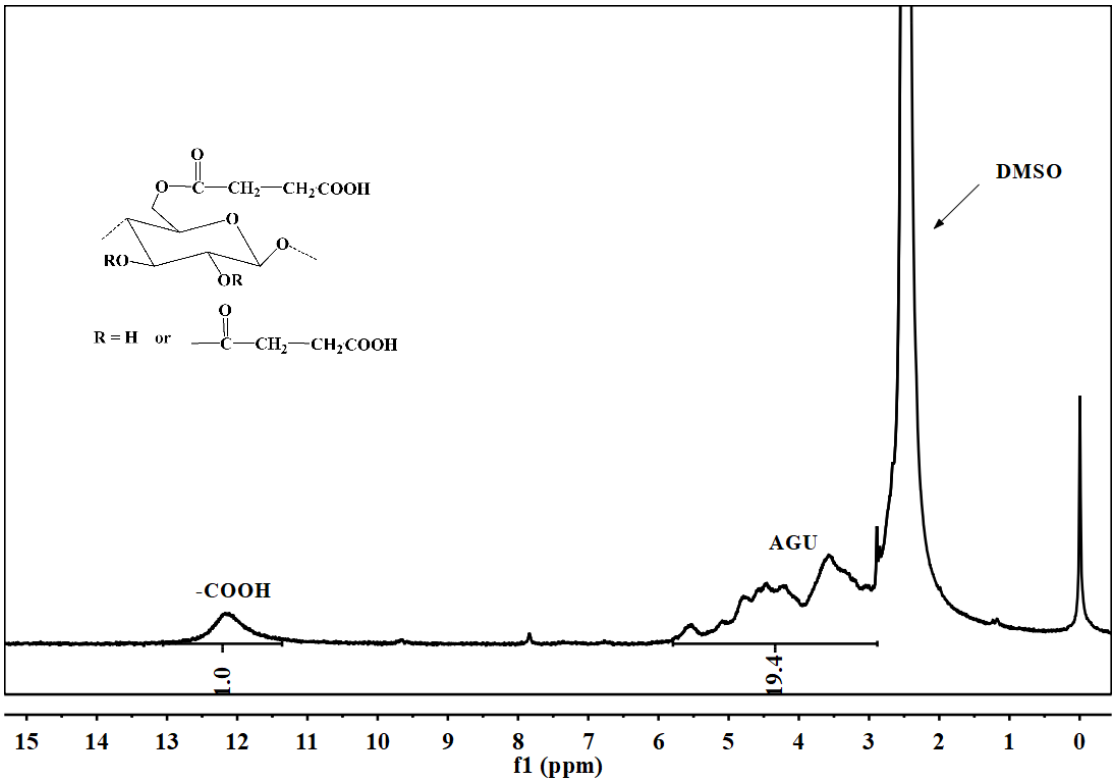

Figure S15. ^{1}H NMR (DMSO-d$_6$) spectrum of CSMEA (C-12, DS =0.36).

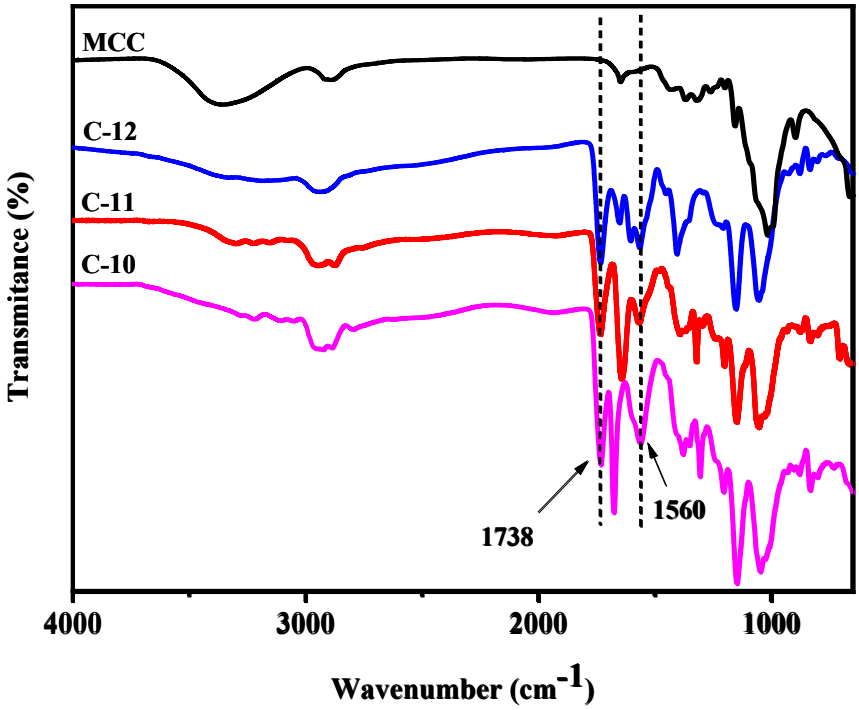

Figure S16. Comparative FTIR spectra of CPILs, C-10 (DS=0.51); C-11 (DS=0.90); C-12 (DS=0.36).

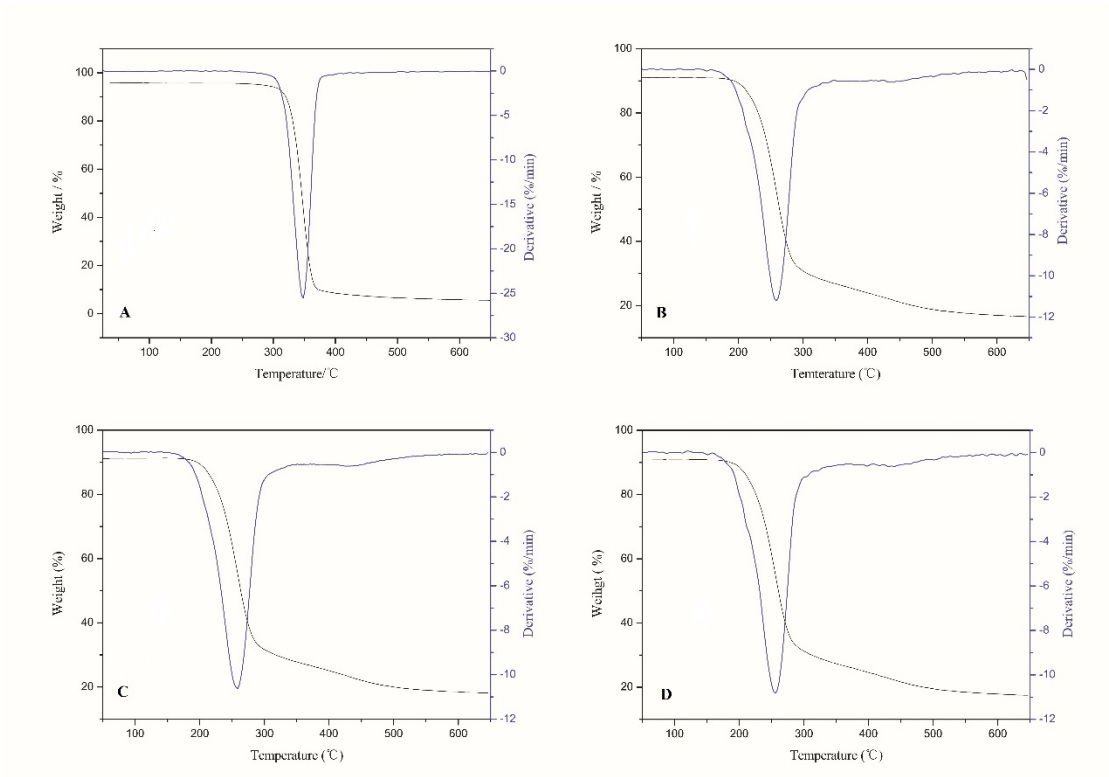

Figure S17. TG and DTG curves of CPILs, (A) cellulose; (B) C-7, DS=1.53; (C) C-9, DS=1.60; (D) C-8, DS=1.64.

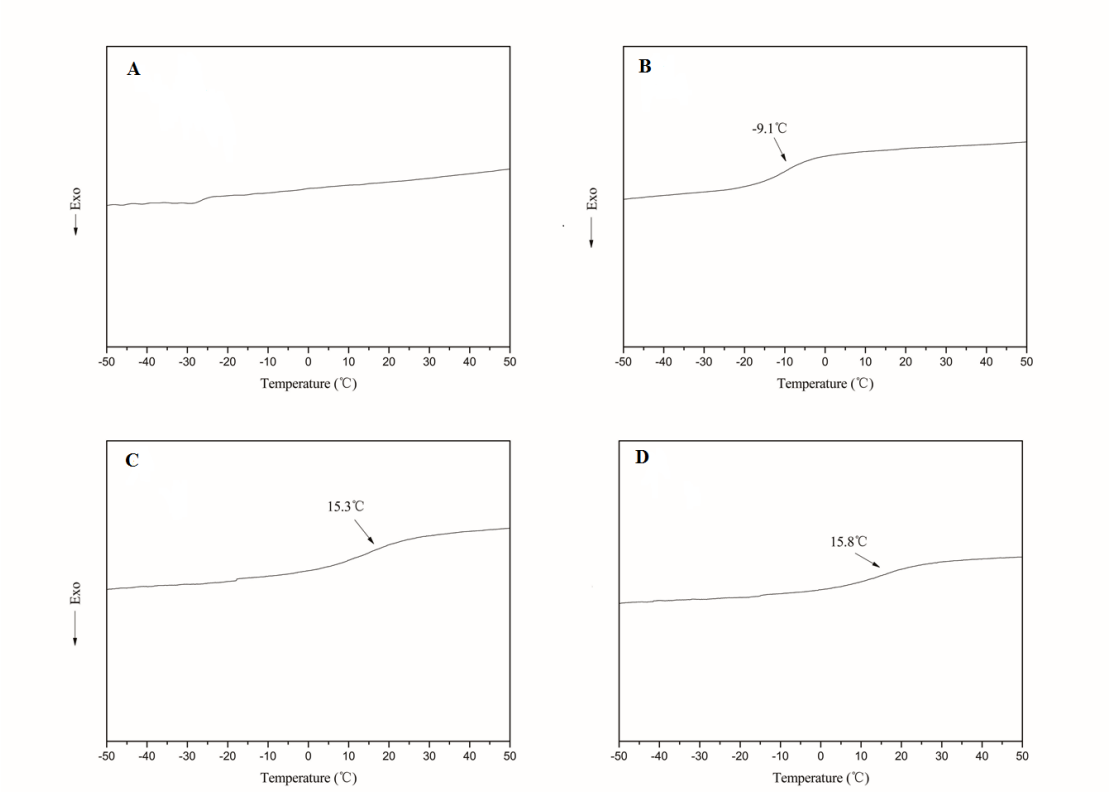

Figure S18. DSC curves of CPILs, (A) cellulose; (B) C-7, DS=1.53; (C) C-9, DS=1.60; (D) C-8, DS=1.64.

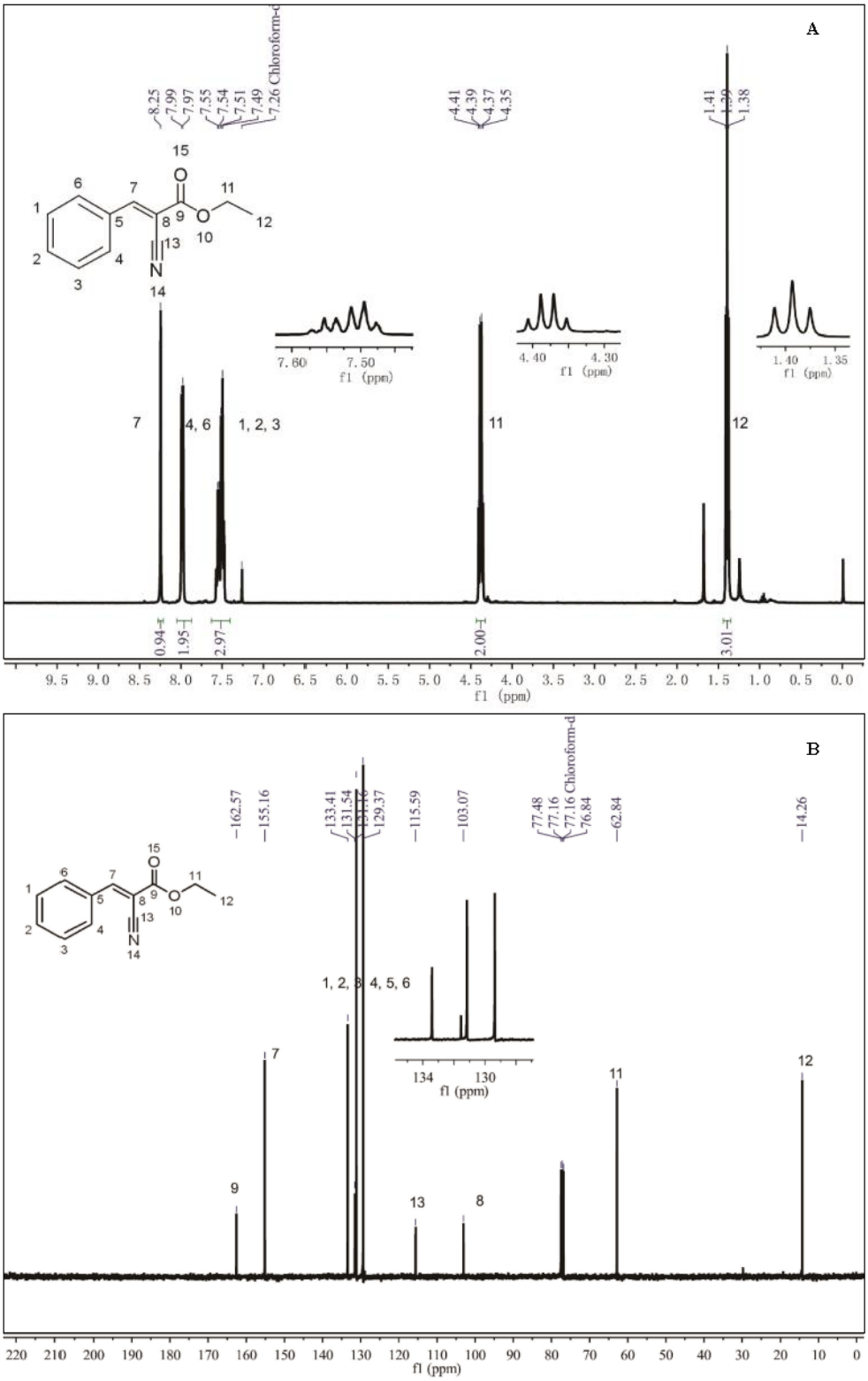

Figure S19. NMR ($CDCl_3$) spectrum of ethyl 2-cyano-3-phenylacrylate, (A) ^{1}H NMR, (B) ^{13}C NMR.

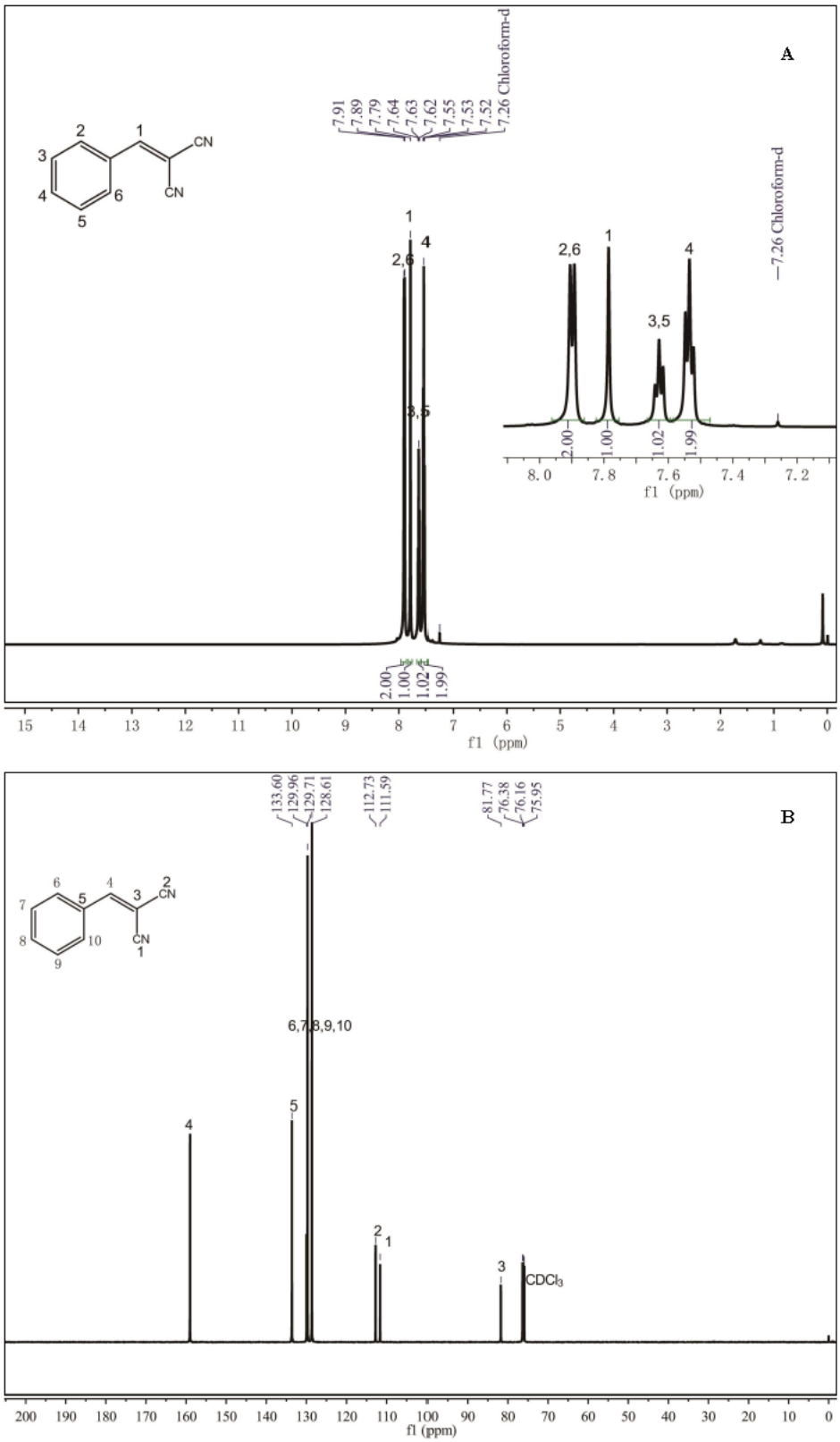

Figure S20. NMR ($CDCl_3$) spectrum of 2-benzylidenemalononitrile, (A) ^{1}H NMR, (B) ^{13}C NMR.

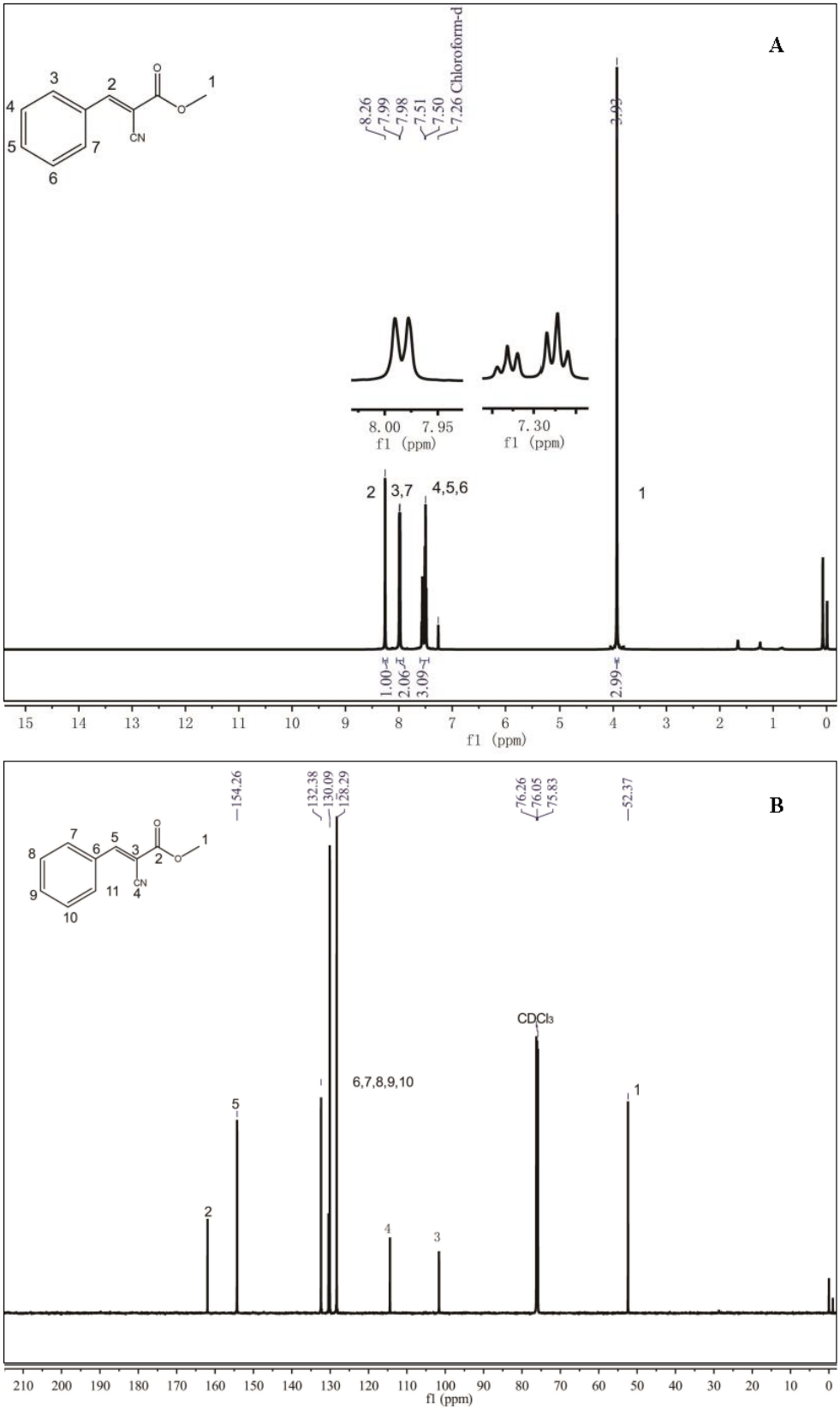

Figure S21. NMR ($CDCl_3$) spectrum of (E)-methyl 2-cyano-3-phenylacrylate, (A) ^{1}H NMR, (B) ^{13}C NMR.

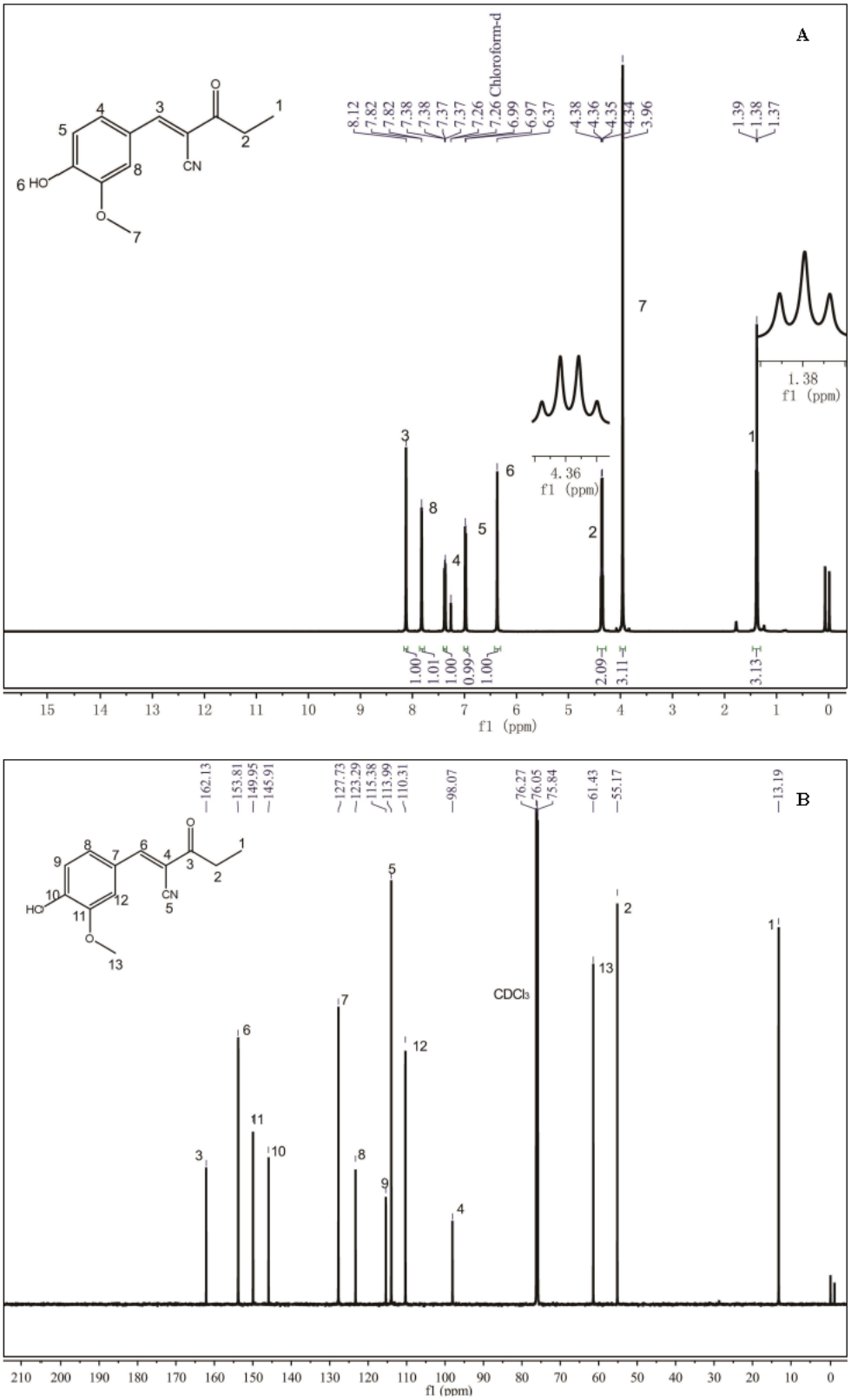

Figure S22. NMR ($CDCl_3$) spectrum of (E)-2-(4-hydroxy-3-methoxybenzylidene)-3-oxopentanenitrile, (A) ^{1}H NMR, (B) ^{13}C NMR.

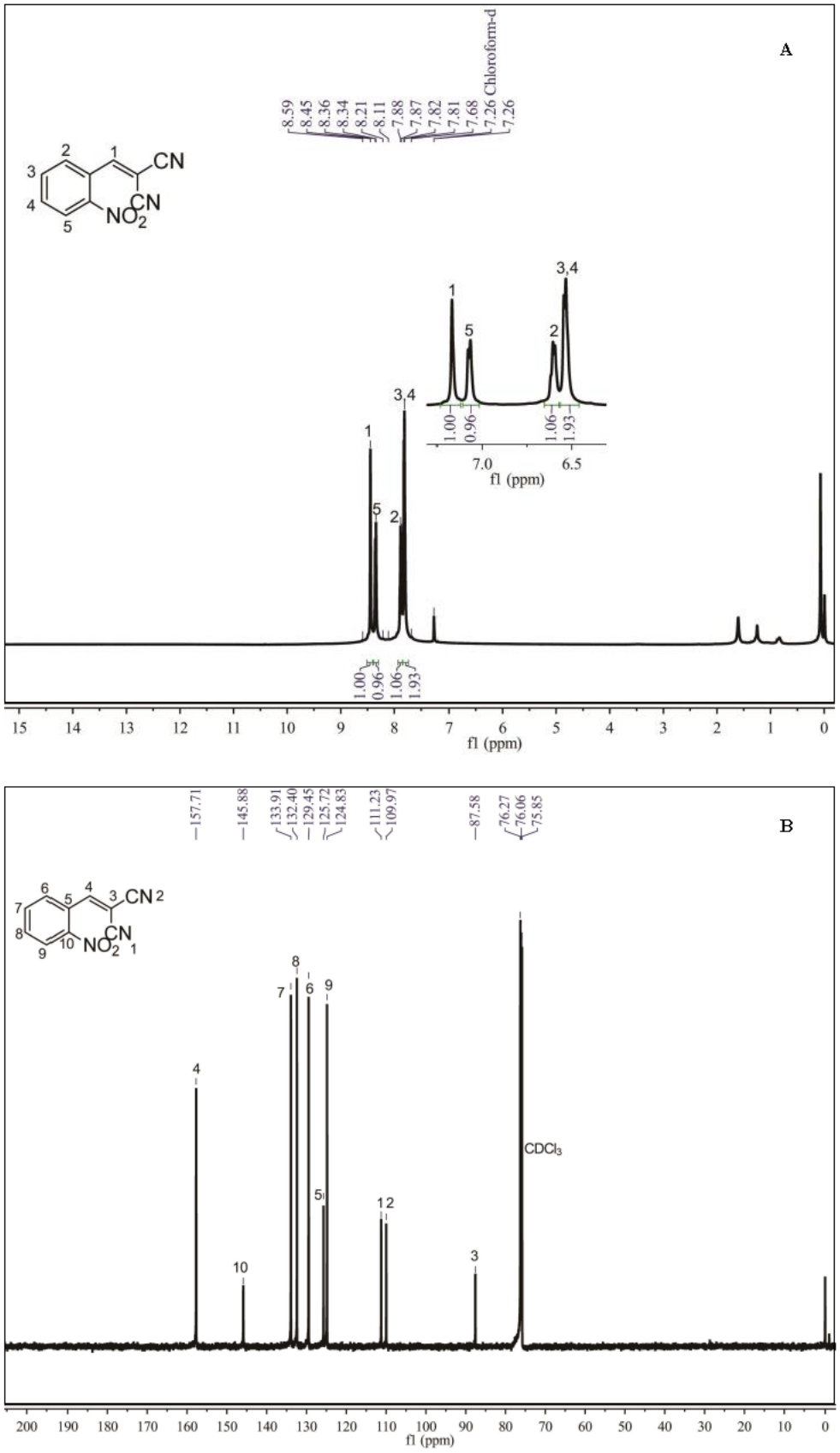

Figure S23. NMR ($CDCl_3$) spectrum of 2-(2-nitrobenzylidene) malononitrile, (A) ^{1}H NMR, (B) ^{13}C NMR.

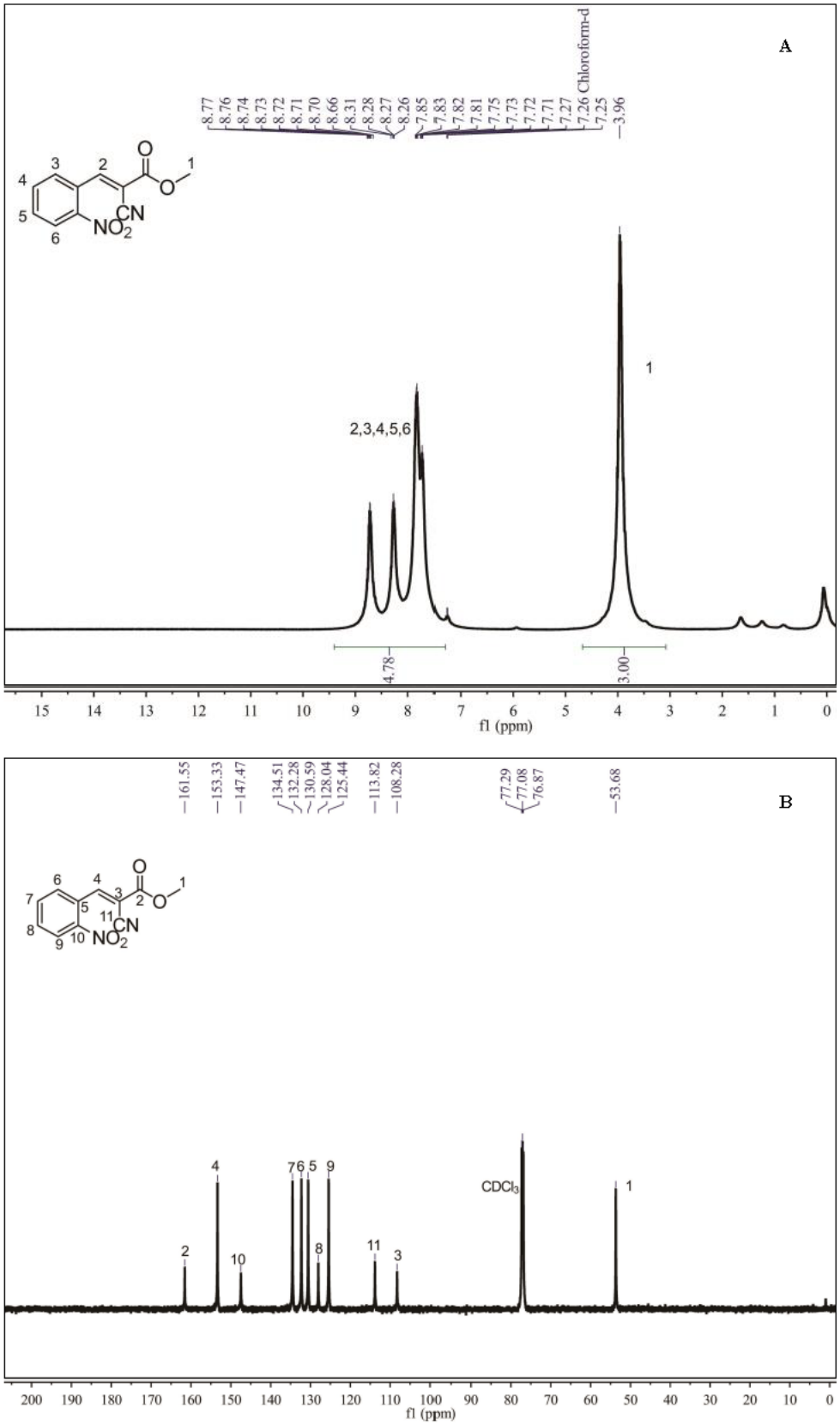

Figure S24. NMR ($CDCl_3$) spectrum of (E)-methyl 2-cyano-3-(2-nitrophenyl) acrylate, (A) ^{1}H NMR, (B) ^{13}C NMR.

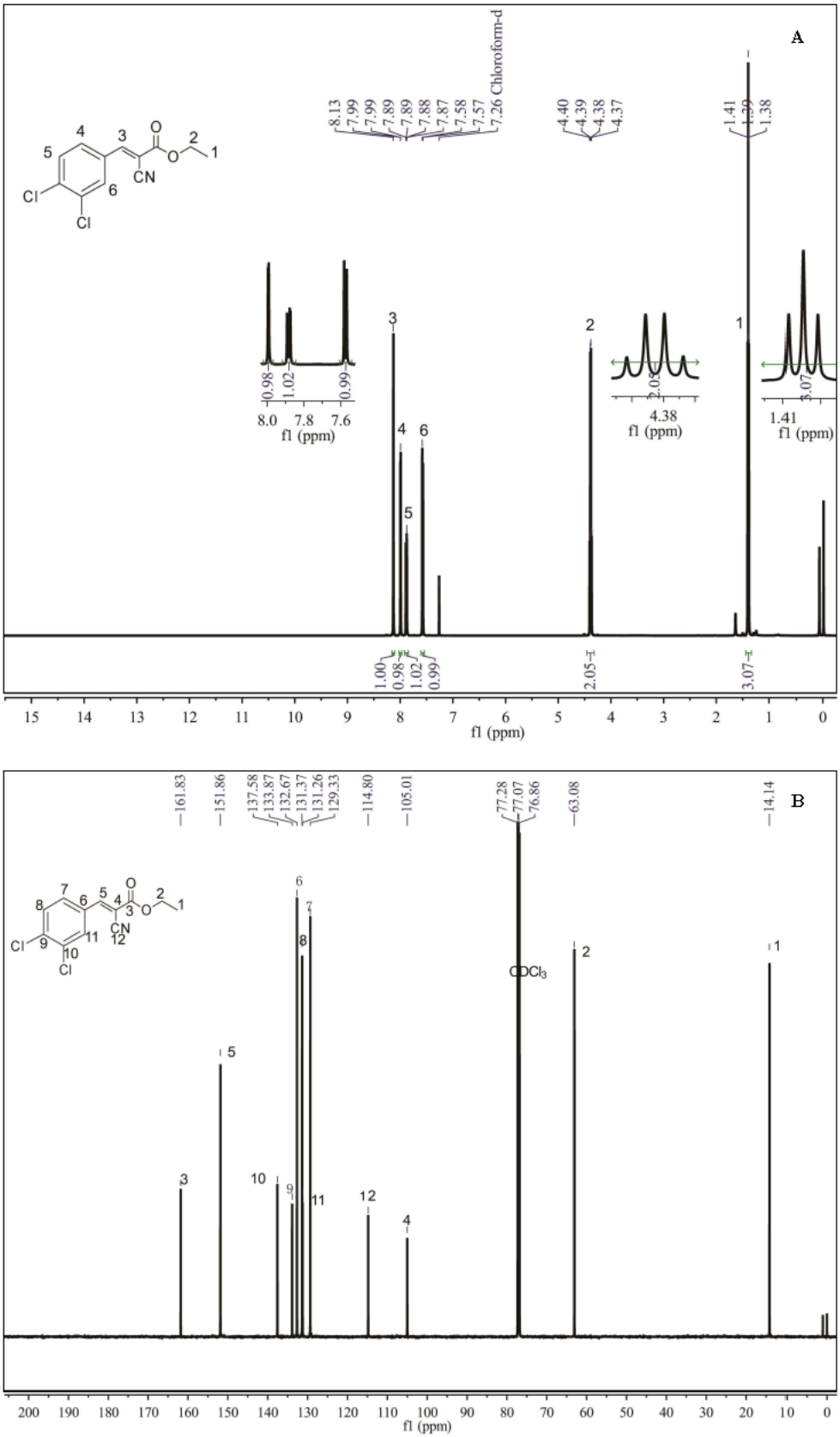

Figure S25. NMR ($CDCl_3$) spectrum of (E)-ethyl 2-cyano-3-(3,4-dichlorophenyl) acrylate, (A) ^{1}H NMR, (B) ^{13}C NMR.

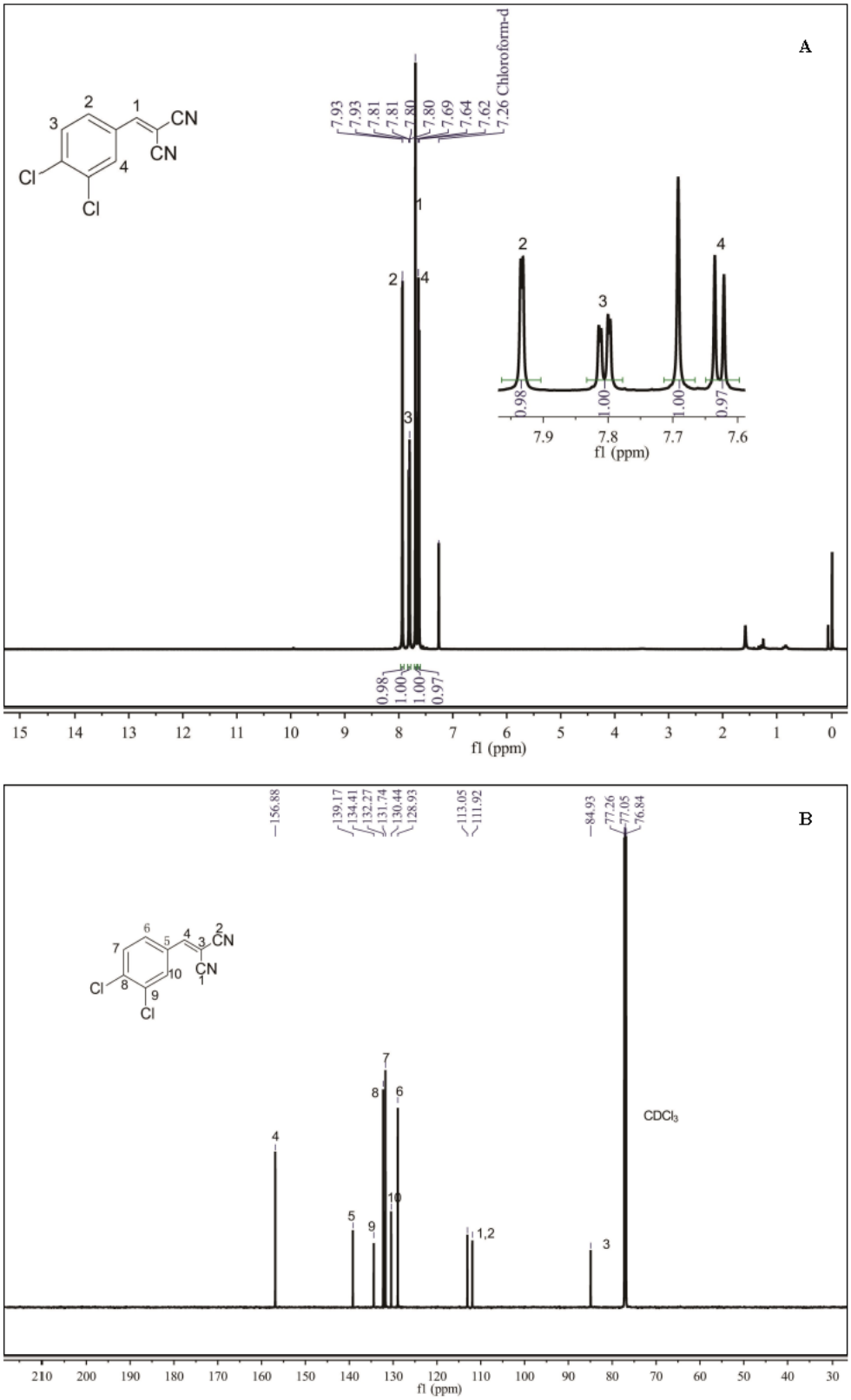

Figure S26. NMR ($CDCl_3$) spectrum of 2-(3,4-dichlorobenzylidene) malononitrile, (A) ^{1}H NMR, (B) ^{13}C NMR.

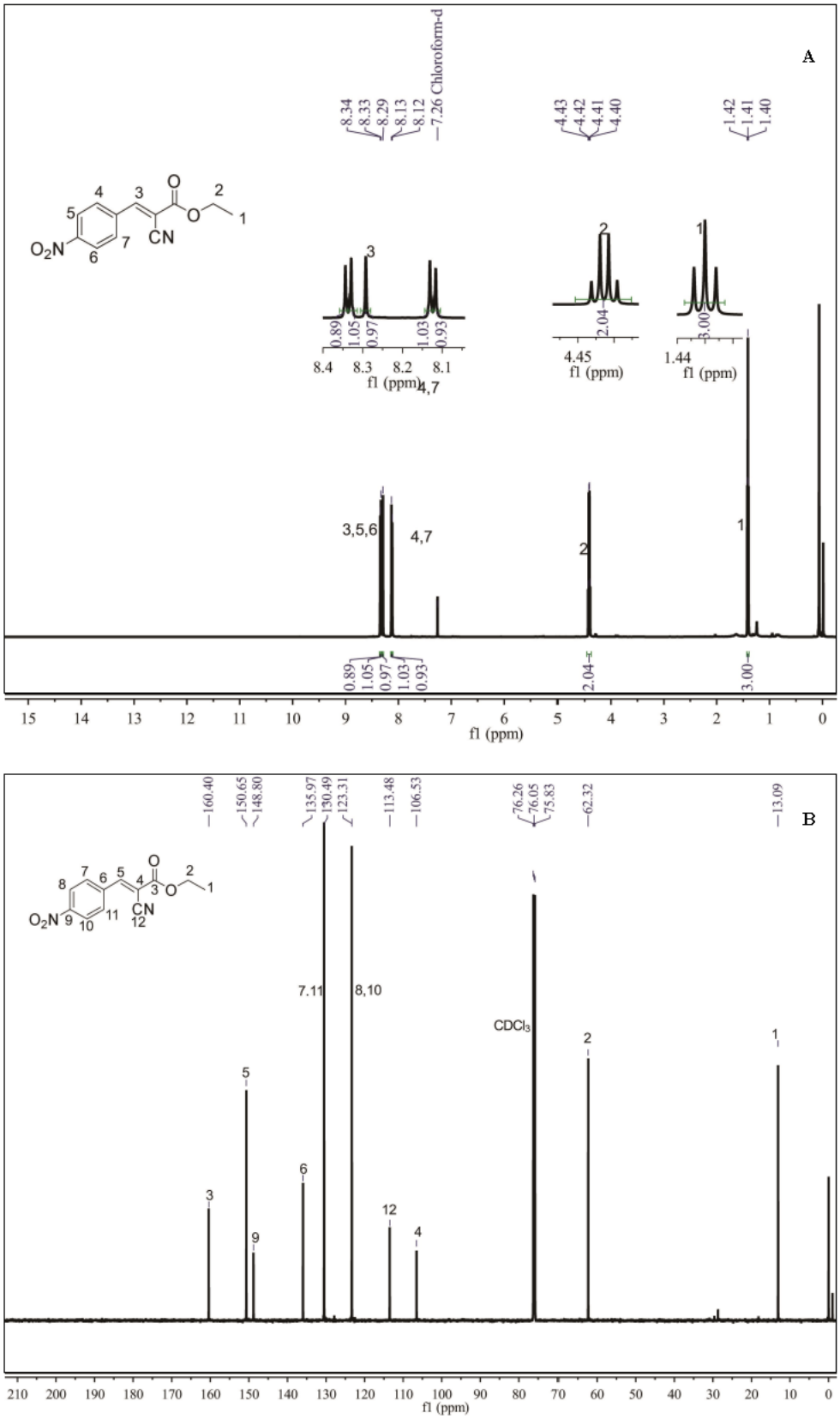

Figure S27. NMR ($CDCl_3$) spectrum of (E)-ethyl 2-cyano-3-(3,4-dichlorophenyl) acrylate, (A) ^{1}H NMR, (B) ^{13}C NMR.

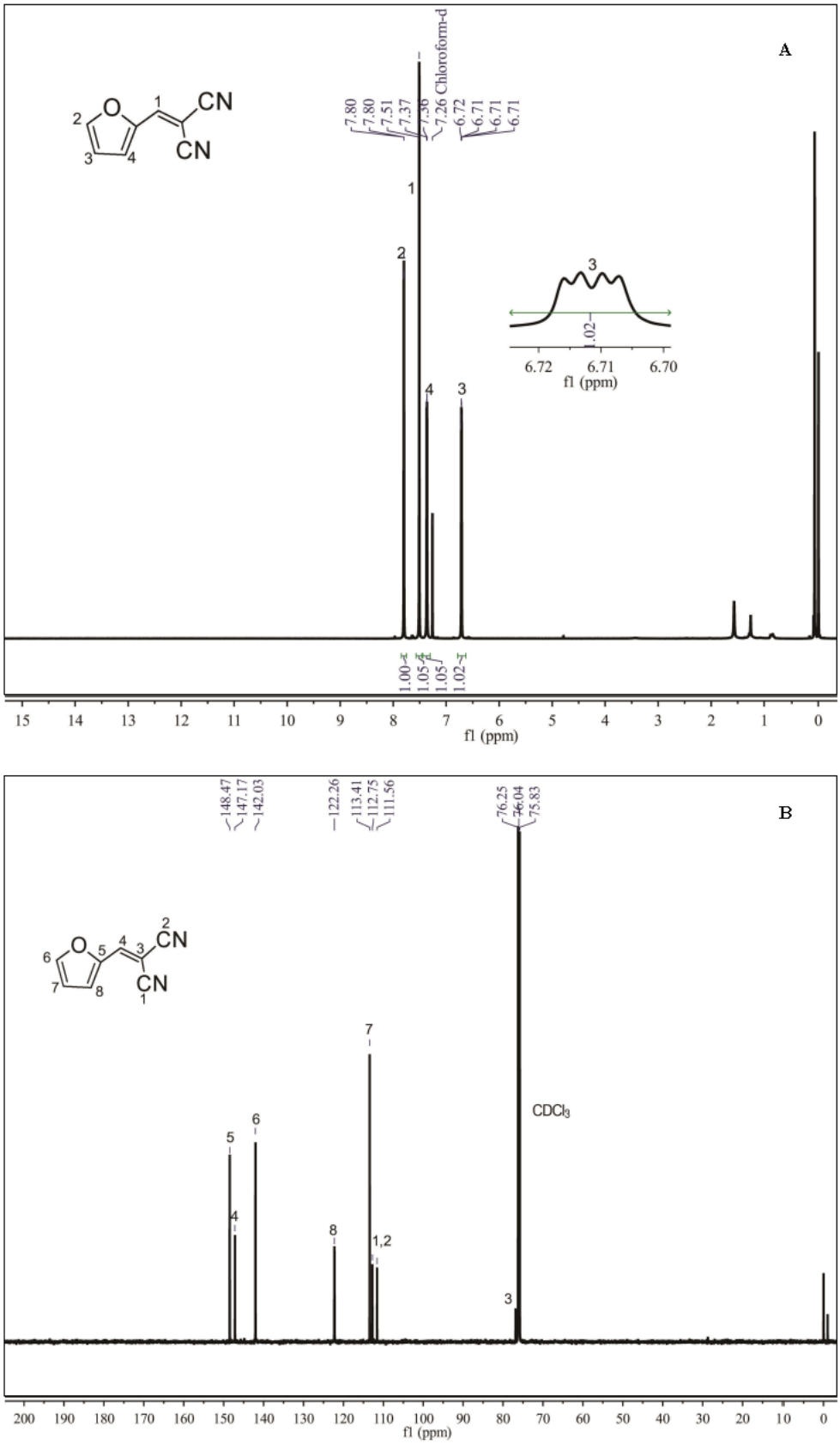

Figure S28. NMR ($CDCl_3$) spectrum of 2-(furan-2-ylmethylene) malononitrile, (A) ^{1}H NMR, (B) ^{13}C NMR.

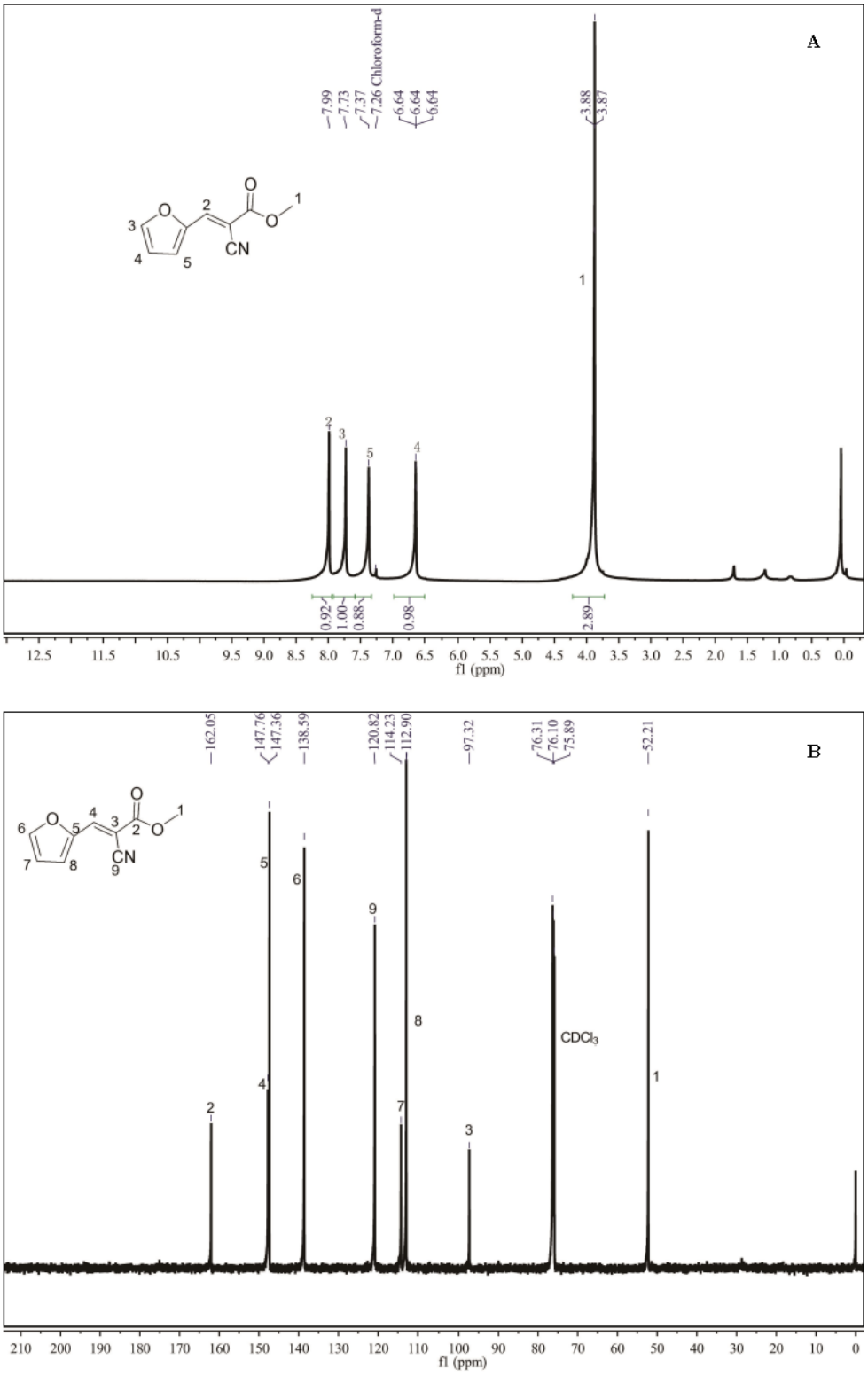

Figure S29. NMR ($CDCl_3$) spectrum of (E)-methyl 2-cyano-3-(furan-2-yl) acrylate, (A) ^{1}H NMR, (B) ^{13}C NMR.

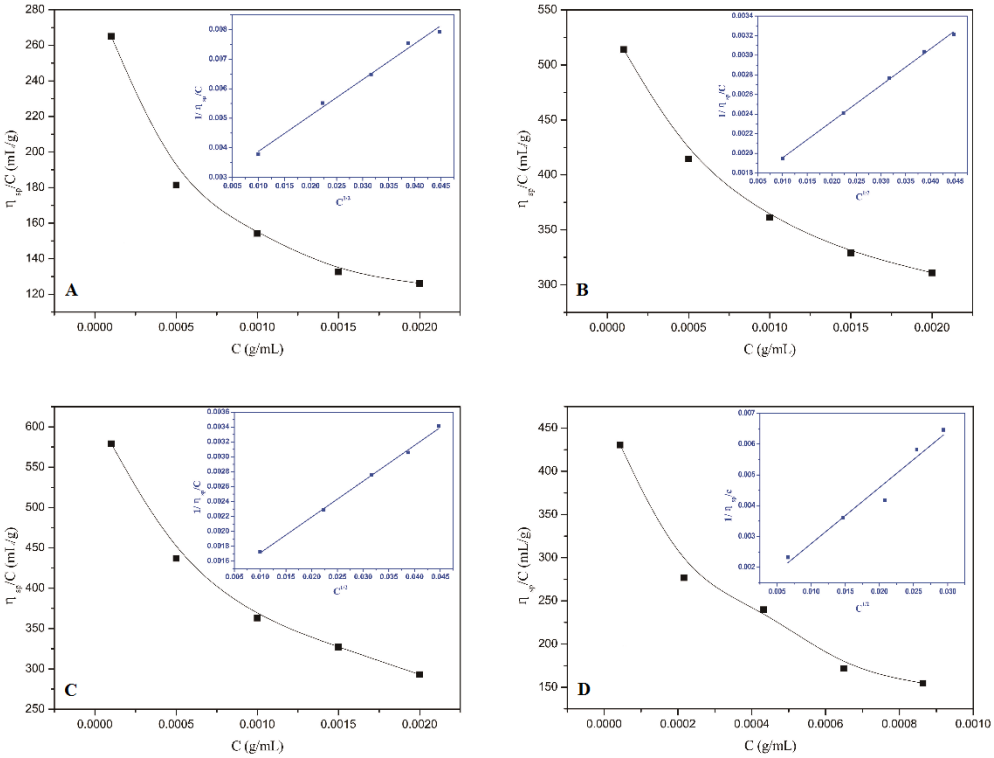

Figure S30. The relationship between reduced viscosity (η_{sp}/C) and concentration (C), A (C-1, DS=1.43); B (C-2, DS=1.57); C (C-3, DS=0.56); D (C-8, DS=1.64). The inset is a linear fit of C/η_{sp} and $C^{1/2}$, 25 °C.

Table S1. Intrinsic viscosity [η] and Zeta potential of CPILs.

Samples	DS	[η] (mL/g)	Zeta potential (mV)
C-3	0.56	376	-14.52
C-1	1.43	633	-26.67
C-2	1.57	813	-30.24
C-8	1.64	1058	-36.04